ADVANCED MATERIALS TECHNOLOGIES
www.advmattechnol.de

# Large Scale Exchange Coupled Metallic Multilayers by Roll-to-Roll (R2R) Process for Advanced Printed Magnetoelectronics

*Preeti Gupta,* Dmitriy D. Karnaushenko, Christian Becker, Ibrahim E. Okur, Michael Melzer, Burak Özer, Oliver G. Schmidt, and Daniil Karnaushenko**

**Till now application of printed magnetoelectronics is hindered by lack of large area exchange coupled metallic multilayers required to produce printable magneto-sensory inks. Large-scale roll-to-roll (R2R) fabrication process is an attractive approach owing to its capabilities for high volume, high throughput, and large area manufacturing. Precise and high performance R2R sputtering technology is developed to fabricate large area giant magnetoresistive (GMR) thin-films stacks that contain 30 metallic bilayers prepared by continuous R2R sputtering of Co and Cu sequential on a hundred meters long polyethylene terephthalate (PET) web. The R2R sputtered Co/Cu multilayer on a 0.2 × 100 m$^2$ PET web exhibits a GMR ratio of ≈40% achieving the largest area exchange coupled room temperature magneto-sensitive system demonstrated to date. The prepared GMR thin-film is converted to magnetosensitive ink that enables printing of magnetic sensors with high performance in a cost-efficient way, which promotes integration with printed electronics. An average GMR ratio of ≈18% is obtained for 370 printed magnetic sensors. The realized precise R2R sputtering approach can also be extended to a wide range of hybrid thin-film material systems opening up a path for new functional inks applied with printing technologies.**

## 1. Introduction

Giant magnetoresistance (GMR) effect has opened the pathway for the new scientific and technological revolution tremendously influencing the magnetic sensors and data storage technologies since the first works of Albert Fert and Peter Grunberg on thin metallic systems.[1,2] The spectrum of GMR based applications has broadened significantly after obtaining deeper insights into underlying physics behind the GMR effect.[3–5] This included but not limited to automotive applications,[6] contactless sensors in aviation and space industry,[7,8] magnetic compasses,[9] and the area of biomedical applications.[5,10,11] However, the wafer scale manufacturing and expensive semiconductor processes hindered the application of magnetic sensors from entering into the printed electronics sector. The most important setback for today's printable magnetoelectronics is low GMR material yield which is limited due to the conventional deposition techniques applied to grow thin-films on a wafer size substrates.[12–14]

In recent decade, flexible, stretchable, and printable technologies have attracted significant attention as an alternative promising pathway due to the possibility to involve additive processes in the manufacturing. Additive manufacturing being environmentally friendly uses less raw materials compared to the conventional subtractive microelectronic processes such as photolithography, etching and deposition techniques.[15,16] Using these benefits, additive manufacturing technologies have led to a breakthrough in the field of smart and intelligent polymer based flexible and printable electronics.[17–20] Thin polymeric substrates have played a crucial role in realizing this new form of electronics by offering low fabrication costs, mechanical flexibility and providing a large working area for manufacturing processes that can be accomplished with high throughput roll-to-roll (R2R) and sheet-to-sheet (S2S) systems.[21–23] Advancements in functional materials and fabrication processes offered new building blocks for electronic circuits e.g. interconnects,[24] transistors and sensors,[25] which became flexible and printable.[26] Printed flexible devices such as gas, temperature, strain and magnetic sensors have gained remarkable attention

P. Gupta, I. E. Okur, B. Özer
Institute for Integrative Nanosciences
Leibniz IFW Dresden
01069 Dresden, Germany
E-mail: p.gupta@ifw-dresden.de

D. D. Karnaushenko, C. Becker, O. G. Schmidt, D. Karnaushenko
Center for Materials Architectures and
Integration of Nanomembranes (MAIN)
TU Chemnitz
09126 Chemnitz, Germany
E-mail: daniil.karnaushenko@main.tu-chemnitz.de

M. Melzer
Bundesanstalt für Materialforschung und-prüfung (BAM)
12205 Berlin, Germany

B. Özer
Institute for Solid-State Physics
Leibniz IFW Dresden
01069 Dresden, Germany

The ORCID identification number(s) for the author(s) of this article can be found under https://doi.org/10.1002/admt.202200190.



**DOI: 10.1002/admt.202200190**

 

due to their noteworthy applications in soft robotics,[27,28] electronic skins,[20] wearable electronics,[29] smart textiles,[30] contactless human–machine interfaces and future bio-integrated consumer electronics[11]. The versatility of printed flexible devices is enabled due to an integrability with different surface geometries which is promising for a range of applications such as liquid level monitors[31] and flexible position sensors.[11] The blending of electronics with printed magnetic sensors offers an additional degree of freedom to explore for example, intelligent and smart packaging, contactless magnetoelectronic systems, and contactless motion and position detection schemes with high sensitivity.[11] Printed flexible magnetic sensorics show high sensitivity and detectivity, low power consumption, good mechanical flexibility, and robustness while relying on the magnetoresistive effect.[11,13]

Printable GMR sensors have already been shown as promising system for obtaining high sensitivity at room temperature on different substrates such as paper, polymer, or ceramic based materials.[13,14] As it has been demonstrated previously, the printed magnetic sensors based on GMR effect[13] possessed high sensitivity and ≈37% GMR on different substrates without affecting the sensor performance wherein, the application of the magnetosensitive ink was proven in the form of an electronic switch.[13,14] Recently, an interesting work on printed stretchable GMR sensors have been reported where the sensitivity, printability, and stretchability parameters of magnetic sensors were discussed with an aim of realizing highly compliant electronics for e-skin and consumer applications.[32] Thus, the most upfront solution is to print magnetic sensing elements at predefined positions on a flexible electronic circuitry or other arbitrary shaped surfaces such as casing and packages.[14] To achieve this, it is of utmost importance to develop a room temperature magnetic elements with high sensitivity and higher throughput in the form of inks, pastes, or paints that can serve as a raw material for printing tools for example, dispensers or spray coaters. Printed magnetic sensors could be of a great potential for applications such as electronic switches,[14] contactless interactive electronics,[32] augmented reality and smart living.[11] However, the high performance and versatility of formulated magnetosensitive inks were still limited by the yield of GMR material. The current yield is quite low (few milligrams) as the fabrication approach is still restricted by the carrier substrate size.[33] In order to achieve the industrial scale applicability and be integrated with printed technology in a large area, the yield of GMR material should be significantly (2 to 4 orders of magnitude) higher, predominantly in grams. However, transitioning from proof of concept to final product involves considerable efforts, larger equipment, and high level of process control. This is particularly challenging when speaking about scaling-up the production of the GMR base material, which is originally prepared on wafers within the semiconductor grade industrial facilities. Utilization of such facilities was crucial when preparing magnetic sensors mainly due to the need in maintaining process uniformity, layer precision, and purity. Thus, the processes involved in such facilities are rather expensive, offering vanishingly small amounts of final material that can be barely used in any real printing application.

This requirement calls for the development of a large-area deposition of the GMR thin-film on a flexible substrate by utilizing R2R coating technique. R2R deposition methods operate, in contrast to the semiconductor facilities, on much larger areas and play a critical role in enabling cost effective production of thin-film coatings on films made of various materials, such as polymers, metals, and flexible glasses. R2R processing is a very mature field and extensively being used in printing and coating industries.[22] Some of the examples include optic coatings, smart cards, sensors,[34] light emitting devices,[22] wearable electronics,[34] energy harvesting devices,[22] and smart textiles.[35] R2R sputter deposition of metallic multilayers on flexible substrates can offer numerous advantages such as large-area and high-yield of precisely deposited magnetic thin-films, compared to the small substrate area for conventional deposition systems. The R2R process also offers flexibility of using a wide range of substrates such as polymeric films, textiles, papers, metal foils, and ultra-thin glasses.[22] Most commonly used polymeric substrates are polyimide (PI), polyethylene naphthalate (PEN) and polyethylene terephthalate (PET).[36] Among them PET provides properties such as relatively high glass transition temperature, tensile strength, low water absorption, and cost.[22,36] This work focuses on the development of the new precise, but simultaneously large area deposition technology that is capable of producing GMR material on regular polymeric films that have not been demonstrated till now. The new technology has an aim of reducing the production cost, time and energy of precise high purity layered stacks, that is, GMR multilayers for printed magnetic sensors. The achieved R2R deposition process has enabled production relevant timelines and production yields which was not possible to achieve before with the semiconductor grade facilities. The advantages offered by the R2R process[22,23,34,37] include but not limited to the reduced material costs, capital and energy expenditure, and production-related labor cost, which is a primary concern for industrial scale applications. In addition, reliability and reproducibility which is one of key factors in large scale production have also been positively affected by controlling the end product quality and specifications.

Here, we present the first fully roll-to-roll processed flexible GMR thin-films with large-area deposition approach providing high-yield of magnetoresistive material. To achieve this, we developed an R2R thin-film magnetron sputtering system, custom designed to deposit precise metal multilayers under vacuum. The developed R2R thin-film sputtering system offers a choice of the web dimension in the length scale where 100, 200, or 300 m long webs can be selected. For the first time, we demonstrate the large-scale, R2R deposition of an exchange coupled metallic multilayer of alternating ferromagnetic (Co) and non-magnetic (Cu) film on a flexible and thin 100 m PET web demonstrating ≈40% GMR effect at room temperature. We achieved the factor of around 10 000 increase in functional deposited area of exchange coupled multilayers fabricated in a single run and a factor of 150 decrease in processing time compared to the conventional 4-in. wafer scale coating approach. The magnetosensitive GMR ink is further formulated and processed to achieve printing of magnetic sensors on large-scale using an A4 size PET substrate with

7 × 20 array of contact pairs. The as-printed 370 GMR sensors exhibit statistically averaged ≈18% GMR value at room temperature. The process of magnetosensitive ink formulation is optimized to achieve consistent batch to batch production of GMR ink cartridges that will also allow end users to have confidence in the final product. In numbers, 100 m GMR thin film deposited on PET is equivalent to 637 × 8 inch (2548 × 4 wafers or 119 days of sputtering, when coating simultaneously 8 wafers at a time) which have been deposited in less than 2 days. The whole process costs have been reduced by around factor 100 from thin film deposition to ink formulation. This included lower personal operating costs (the process is fully automatic), better machine utilization (24 × 7 operation circle, lower number of venting/evacuation circles), highly optimized process, and solvent recovery that have been addressed to ensure the low production cost of the end product without affecting its performance. We believe that the developed R2R manufacturing process for GMR thin film will accommodate the need of industrial demands for high yield of magnetic element desired for integrating hybrid magnetoelectronic systems with printing technology such as contactless, intelligent, and smart electronic devices in future.

## 2. Results and Discussion

### 2.1. Roll-to-Roll Thin-Film Deposition System

The modular R2R deposition system is designed to fabricate precise material multilayers base pressure down to $5 \times 10^{-6}$ mbar on flexible as well as rigid substrates. The key feature of

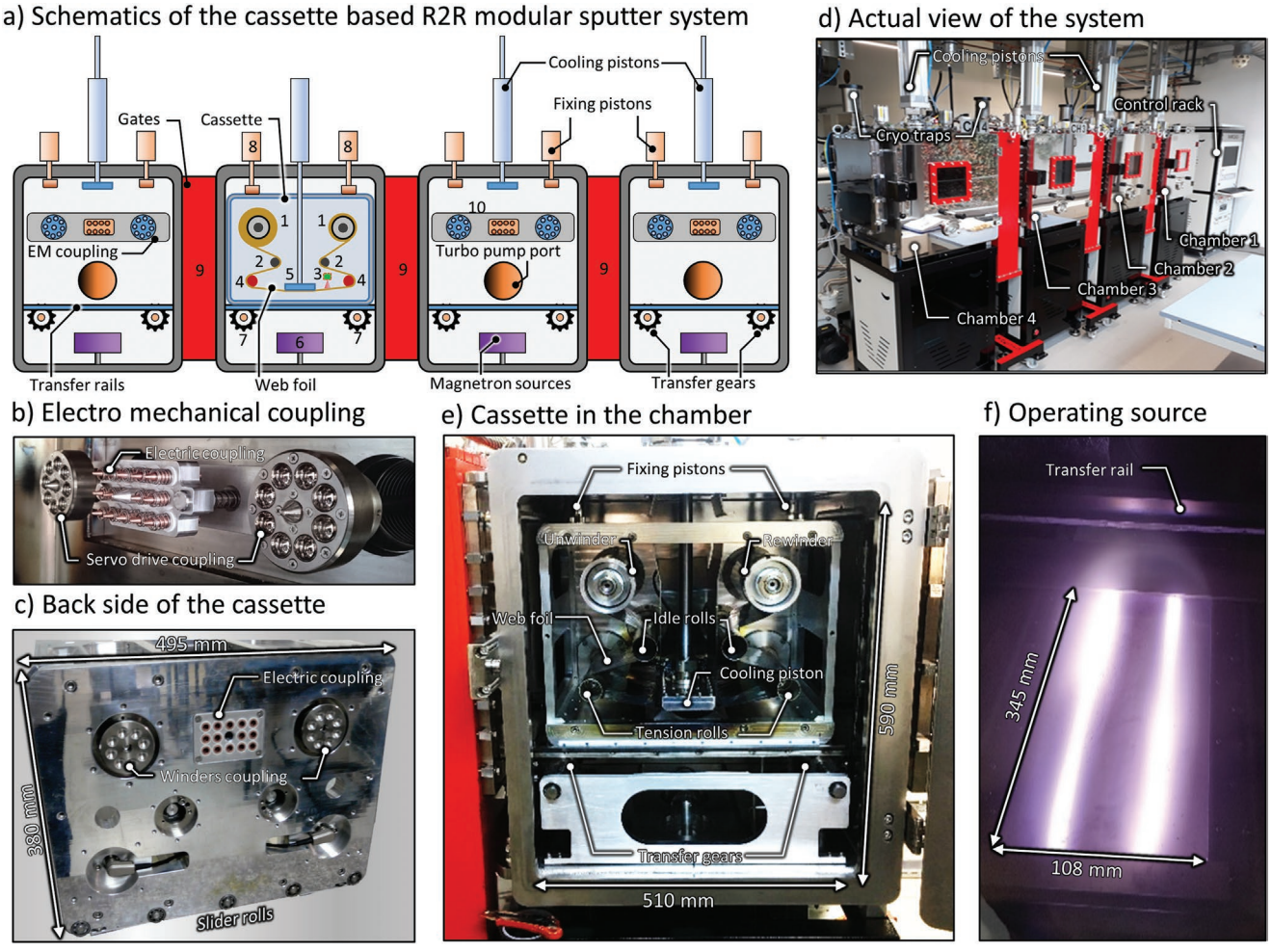


**Figure 1.** The modular roll-to-roll deposition system with a movable cassette. a) Schematic of the deposition system consisting of four deposition chamber modules, which are isolated from each other with gates. Cassette inside the chamber with the roll-to-roll foil transfer system consisting of 1) web foil rolls, 2) idle rolls, 3) bar code scanner, 4) tension rolls. Each chamber is equipped with 5) cooling piston, 6) deposition source, 7) transfer gears and rails, 8) cassette fixing pistons, and 9) chamber isolation gates. b) The cassette is coupled with the chamber through an electromechanical coupling mechanism 10) consisting of electric spring-loaded contacts and mechanic spring loaded servo driving shafts for unwinder and rewinder. c) The electromechanical coupling is fit with the cassette's backside coupling electric and mechanic ports. d) Photograph of the actual system. e) Cassette within the chamber with mounted web foil and the extended into the cassette cooling piston. f) Operating source with plasma generation during the deposition.

the system is a mobile cassette, containing the entire web materials that moves among four stainless steel (SAE 304 grade) vacuum chambers isolated by three electro-pneumatically actuated transfer gate valves (**Figure 1**a). The R2R cassette designed here is made up of aluminum and is transferred by means of gears through the linear chamber system using rails (with bearing rolls or friction sliders). During the deposition, only the active chamber (housing with the cassette) is operating for deposition of a particular material while the other chambers are insulated from each other, which avoids cross contamination and keeps the vacuum at lowest base pressure. The cassette integrates all of the necessary rolls for operation such as two tension sensor rolls, idle rolls, winder and rewinder, which carry the actual PET foil. The cassette mechanics relies on the female cassette side clutch roll mechanism (Figure 1c) to lock itself to the male clutch of the chamber (Figure 1b) during the deposition. This mechanism is driven externally though the vacuum feedthrough with a pair of servomotors on each chamber back side. The embedded sensors are connected through the vacuum electro-mechanical contactor integrated in the cassette and in each chamber of the deposition system (Figure 1d).

The R2R operation principle depends on the electromechanical system which transfers the web from the unwinder roll to the rewinder roll within the cassette located in one of the chambers (Figure 1e). The web is pulled at a specific constant speed, which is controlled by the servo motors, while optic speed and tension sensors integrated into the cassette controls tension of the web foil and its speed. Once the cassette with the PET web is loaded into the load-lock chamber, it starts rolling slowly with the speed of 300 cm $min^{-1}$ under the vacuum for outgassing (20 h for the 50 µm thick 0.2 × 100 $m^2$ PET foil roll) until the pressure has reached $5 \times 10^{-6}$ mbar at which the deposition can be started. Upon reaching the desired base pressure an adjacent chamber is actively pumped and the gate valve opens to allow the transfer to the desired chamber for the next processing step. Then the cassette is coupled to this chamber electrically and mechanically, and the gate closes.

When the coupling and gate closing process is accomplished the cooling piston penetrates the cassette interior from top to bottom of the cassette pressing the web toward the magnetron (Figure 1e), rolling starts and plasma ignites (Figure 1f) beginning the deposition process until the desired web section is coated with the preset material thin-film. Then the cassette is decoupled and the cooling piston is removed from the cassette interior. The gate valve is then opened for transferring the cassette to another chamber repeating the whole process by depositing another material and layer. The whole system is designed for a semi-automatic operation which is controlled with the software and graphical user interfaces. The receipt is loaded in the control software and sputter deposition of desired multilayers is carried out automatically. The system is capable to sputter metals, insulating ceramics and semiconductors by using DC and RF magnetron sources. Each chamber is equipped with mechanical (35 $m^3$ $h^{-1}$) and turbo molecular pumps (2520 $m^3$ $h^{-1}$) to achieve the desired vacuum level. The pressure in each chamber is red by three gauges: cold cathode gauge (760–$10^{-9}$ Torr), Pirani gauge (760–$10^{-3}$ Torr), and ceramic capacitance gauge (0.1–1000 Torr). It is noticeable that the overall R2R mechanics consists of a few rolls in this design required for the feedback controlled unwinding and rewinding operation. The number of chamber modules in such system grows proportionally with the number of required targets and can be configured on demand (Figure 1d consists of four chambers). The system can be designed and extended by adding new chambers without altering the already existing modules. This is an obvious benefit compared to conventional R2R systems that are fixed in design, require numerous rolls and the volume and complexity of the system exponentially grows with the number of targets.

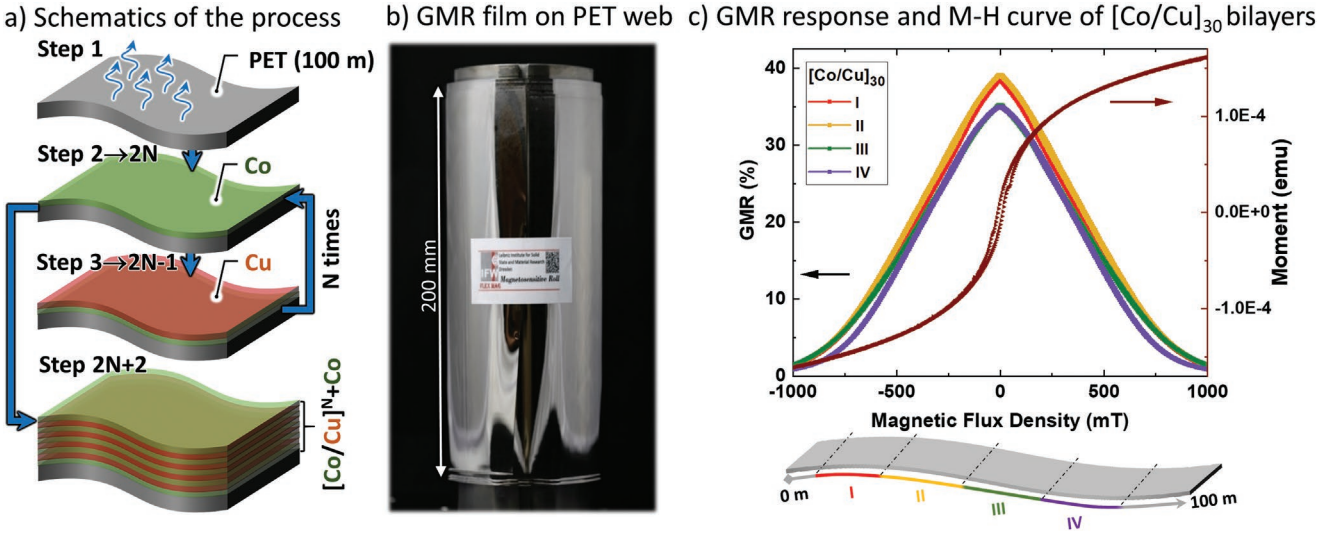


**Figure 2.** Giant magnetoresistive thin-films on polyethylene terephthalate web. a) Schematic representation of Co/Cu multilayer deposition process on the PET web by R2R magnetron sputtering. b) Magnetosensitive R2R deposited GMR multilayer on 0.2 × 100 $m^2$ PET web. c) GMR response at each 20 m along 100 m of the web and *M–H* curve of $[Co/Cu]_{30}$ multilayer. The schematic represents the roll sections measured every 20 m.

### 2.2. R2R Deposition of Co/Cu Multilayer on Flexible PET Web

The multilayer thin-films of cobalt (Co) and copper (Cu) are deposited on the surface of 100 m long PET web (**Figure 2**a) using magnetron sputtering technique. The 100 m long PET web is loaded in the cassette that is positioned in the chamber 1 (CH1). After loading, the PET foil is degassed under the vacuum for 20 h until the base pressure reaches $5 \times 10^{-6}$ mbar value. During this process, the web is continuously unwound and rewound with the speed of 300 cm $min^{-1}$ for 10 cycles with filled liquid nitrogen cryogenic traps. The complete cassette with the PET web is transferred from one chamber to another for the deposition. First the cassette goes to the chamber 3 (CH3) containing cobalt, and then to chamber 2 (CH2) containing the copper source and then back to the CH3 repeating the deposition cycles, with the last layer of cobalt deposited at the very end of the process. These alternating ferromagnetic (Co) and non-magnetic (Cu) layers are grown at room temperature with an argon process pressure of $7 \times 10^{-3}$ mbar. Once the deposition of individual metallic layers is over, the cassette returns back to the CH1. The initial and the last 3 m long sections are labeled with the "Start" and "Stop" barcodes on the backside of the web which determine the start and stop position of the multilayer section respectively. The software recognizes these labels with an integrated barcode scanner in the cassette (Figures 1a–**3**) to perform the automatic process. After the start code is recognized, the deposition starts by igniting the plasma and winding the web till the stop position is recognized on the foil. The web section between the start and stop positions contains the deposited film. Additionally, it is also possible to define different deposition section with different parameters such as speed, power, or thickness of layers etc. To ensure that the layers are coupled in the first antiferromagnetic maximum, the thickness of Co (≈1 nm) and Cu (≈1.2 nm) layers were optimized. The whole process is fully automatic and controlled by the software. The GMR stack with $[Co/Cu]_{30}$ bilayers on the rewound 100 m long PET web is then removed from the cassette (Figure 2b) for magnetoelectric characterization and preparing the ink. Figure 2b shows the appearance of the roll after the deposition, where one can see the shiny metallic coating on the foil surface.

To understand and ensure the deposition homogeneity of the deposited film along the 100 m web, the first and the last 10 m of the foil is cut off, while the remaining foil is separated in sections every 20 m. These sections are measured revealing GMR response by changes in its resistance with

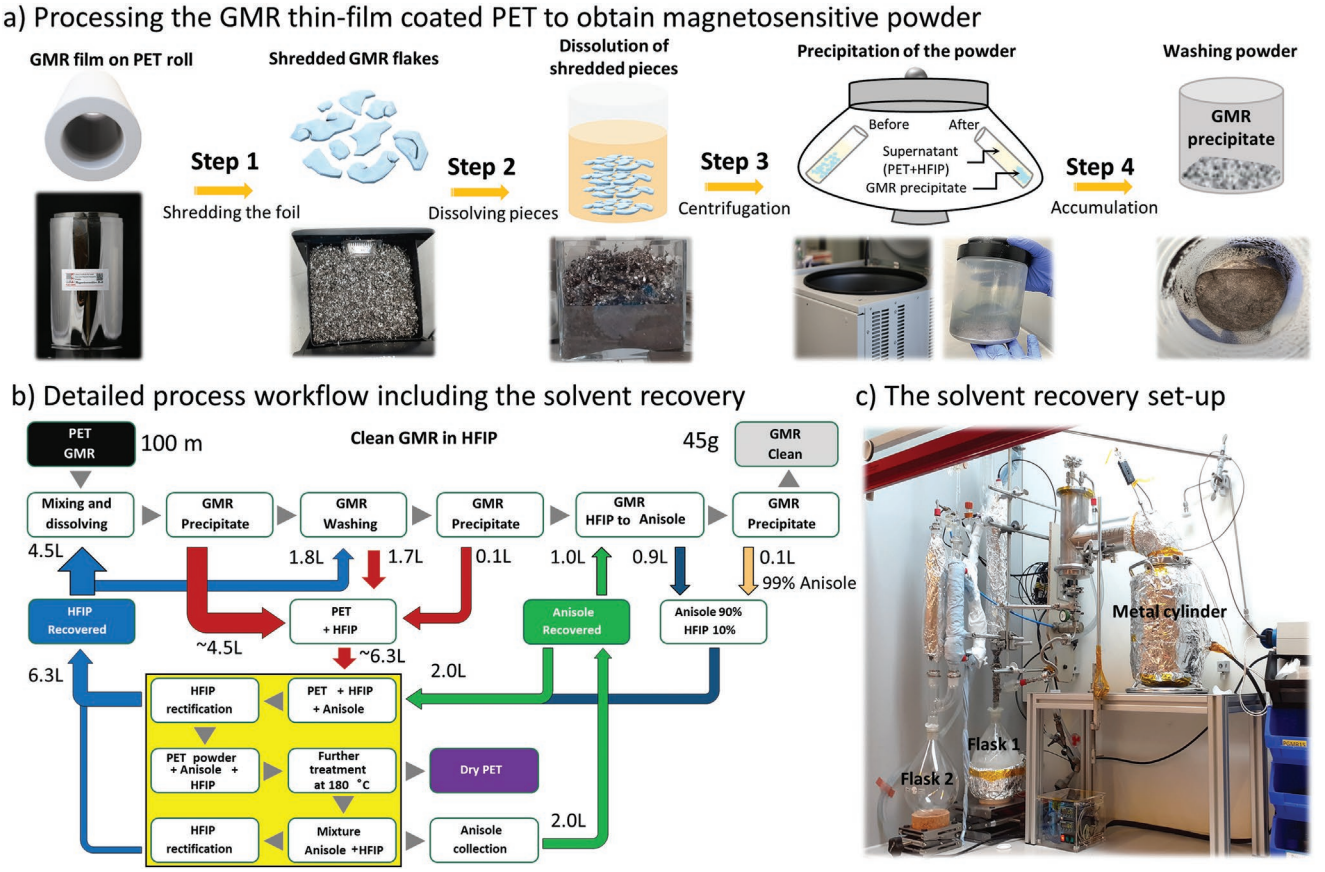


**Figure 3.** Delamination process of the GMR thin-film from the PET foil which includes: a) shredding the magnetosensitive foil, dissolving the foil pieces in HFIP solvent, followed by centrifugation to precipitate the GMR powder and a final washing to accumulate the final product. b) Detailed process workflow that involves the solvent recovery process of the contaminated HFIP with PET and anisole. c) The home-built solvent recovery and rectification set-up.

the standard four-point method with respect to an applied external magnetic field. The magnitude of the GMR effect is characterized by the ratio given by magnetic field dependent change of the sample's resistance, $R$ ($H_{ext.}$), normalized to the resistance value of the magnetically saturated sample, $R_{sat}$: MR ($H_{ext}$) = [$R$ ($H_{ext}$) − $R_{sat}$]/$R_{sat}$. The measured GMR ratio for deposited foil is found to be ≈38%, ≈40%, ≈34%, and ≈35%, for the four different roll section respectively along with saturation field (1000 mT) observed in $M$–$H$ curves of $[Co/Cu]_{30}$ multilayers as shown in Figure 2c. The GMR ratio obtained for different roll sections showed similar GMR value with a little deviation implying good homogeneity of deposited GMR multilayer stacks across the web. The observed GMR ratio of ≈40% on a 100 m long PET is in contrast to the previous works demonstrating 50 bilayers of $[Co/Cu]_{50}$ with GMR ratio of 55% deposited directly on silicon or polymer covered Si wafers,[12–14] concludes the high quality of the deposited thin-films. The value of the GMR effect depends on various factors. For instance, increasing number of bilayers from 8 to 30 improves the GMR effect. The improvement of the GMR effect is due to enhanced scattering at Cu/Co interfaces. However, no improvement has been seen when the number of bilayers has further increased in our system due to loss in interface integrity for outermost layers. The lower value of the GMR effect observed can be attributed to the reduced number of bilayers deposited in this work, scratches on the surface of the foil and the impact of winding and unwinding in each single layer deposition. The sensitivity directly depends on the GMR ratio and inversely on the saturation field. The higher GMR ratio can be obtained by considering the various factors such as individual layer thickness, number of bilayers, and choice of thin film materials while low saturation field can be obtained by choosing softer magnetic materials and optimizing Cu spacer thickness coupling adjacent ferromagnetic layers to higher order antiferromagnetic maximum. This lowers the saturation field and improves the final sensor responsiveness. In this work, the thickness of Cu layer is selected to obtain strong exchange coupling between the two adjacent Co layers coupling them into the first antiferromagnetic maximum for higher GMR ratio.[38] To reduce the saturation field further, different material can explored such as $[Ni_{80}Fe_{20}/Cu]_N$ however negatively affecting the GMR value.[32] Thus, it is important to find a balance between saturation field and GMR ratio for high performance printed GMR sensors with an aim at applications such as consumer electronics or industrial appliances.

The large surface area of the magnetosensitive functional thin-film overcomes the low yield obstacle and processing time scale (32 h for deposition on 100 m web) previously existing when regular wafers were used for manufacturing printable magneto sensory materials. Hence, this work presents a major milestone achieved in the field of printable magnetic sensorics relying on GMR thin-films. These thin-films are further processes to produce magnetosensitive inks or pastes that can be printed or coated on any substrate ranging from silicon, plastic, ceramic, paper, and glass to name a few.[13,32] The full 100 m magneto sensitive foil with deposited GMR stack is used as an initial raw material for the production of magnetosensitive powder and a final ink.

### 2.3. Delamination of the GMR Thin-Film from the PET Substrate

Figure 3a shows the preparation steps of magnetosensitive powder from 100 m PET roll coated with $[Co/Cu]_{30}$ GMR multilayers. The coated foil is shredded into small pieces using a commercially available paper shredder (Figure 3a step 1). The collected shredded pieces are then transferred to a glass container where these coated PET pieces get dissolved (Figure 3a step 2) in hexafluoroisopropanol (HFIP), which is an excellent solvent for dissolving polymers such as polyesters like PET.[39] In the previous works the sacrificial polymer was dissolved in acetone.[12,14,33] A part of shredded pieces is dissolved with HFIP and glass rod is used for mixing to ensure the complete coverage and faster dissolution. Followed by constant stirring, more and more shredded pieces are added to the solution until the full 100 m web is completely dissolved, releasing the coated GMR multilayer thin film as free-flowing flakes inside the PET and HFIP solution. The obtained suspension (magnetosensitive powder, PET, and HFIP) is then distributed among the six centrifuge bottles, each having capacity of up to 1 kg. The mixture is then centrifuged (Figure 3a step 3) using a floor standing refrigerated centrifuge Sigma 8KS at 3000 rpm for 1 h 30 min. After the centrifugation process, the supernatant, the mixture of dissolved PET and HFIP solvent, is collected and stored for further recovery of the HFIP solvent. The obtained magnetosensitive powder precipitate (Figure 3a step 4) is washed several times with fresh HFIP and anisole solvent to ensure the complete removal of the dissolved PET. The as-obtained magnetosensitive powder is further rinsed and cleaned (3 cycle) with anisole. After the final cycle, the magnetosensitive GMR powder is dispersed in a clean anisole for further storage to avoid their oxidation, agglomeration and drying.[13,33] The amount of anisole used for dispersing and storing is adequate enough to only dampen the magnetosensitive powder. The as obtained magnetosensitive powder followed by delamination and purification consists of GMR flakes of different shapes and sizes,[13,14,33] and further used to prepare the magnetosensitive ink.

The supernatant, HFIP solvent with the dissolved PET, obtained during the delamination process then undergoes a solvent recovery and rectification process (Figure 3b) using homemade solvent recovery set up (Figure 3c). Although HFIP is the best suited solvent for PET dissolution, the high cost of the solvent (1 kg—£ 99.00 Fluorochem UK) limits its wide use. Moreover, HFIP+PET serves as a waste product which is not environmentally friendly and is classified as corrosive and hazardous to human health. For these reasons, the used HFIP solvent has to be recovered by double distillation process under vacuum from a mixture enriched with HFIP and dissolved PET. During the centrifugation process, to obtain GMR precipitate, 4.5 L of HFIP solvent is required to dissolve 100 m GMR thin-film coated PET. The GMR precipitate is further washed with 1.8 L of clean HFIP followed by cleaning with 1 L of anisole. The collected 6.3 L of supernatant after centrifugation (which is the mixture of HFIP and PET) is mixed with 2 L of anisole, transferred to a metal cylinder (Figure 3c) and treated at 180 °C under vacuum. The chiller is set at 5 °C and cold water circulates across the vapor condenser connected to collecting flasks 1 and 2 and reflux condenser in the rectification column (Figure 3c) for the maximum solvent recovery. The mixture of HFIP and anisole is collected in flask 1 which further undergoes rectification

treatment at 100 °C under vacuum. The HFIP solvent is then recovered into the flask 2 (6.3 L) and the remaining solvent in the flask 1 is post recovered with anisole (2.0 L) (Figure 3c). After the solvent is recovered completely, the PET precipitate is collected in the metal cylinder which is then removed and stored. This PET precipitate can be in principle further recycled to produce a clean PET foil and closeup turnaround cycle of the GMR powder production. The recovered HFIP and anisole solvents are then further reused without degrading in quality.

### 2.4. Magnetosensitive Ink Formulation

The magnetosensitive powder must be in a carrier fluid wherein, the carrier fluid comprises of solvent and a binder with a high loading (60%) of GMR powder to achieve significant performance of the printed magnetoresistive sensors. The choice of binder can be mono or dual component. The polymer-based binder with a low glass transition temperature is the best suited for printed GMR sensor response.[33] We choose polyepichlorhydrin (PECH) polymer for preparing the binder solution as to provide good electrical percolation between the flakes of printed magnetosensitive ink.[33] The binder solution is made up of polymer, PECH dissolved in an ethyl acetate solvent. The solution is stirred at 400 rpm at 50 °C for 12 h giving PECH binder solution and then filled into 3 cc cartridge for further use as shown in **Figure 4**a.

The magnetosensitive ink is then formulated using the prepared PECH binder (Figure 4b). First, the magnetosensitive powder is cleaned with ethyl acetate to replace anisole for the continuity of the ink formulation process. Then, another 3 cc

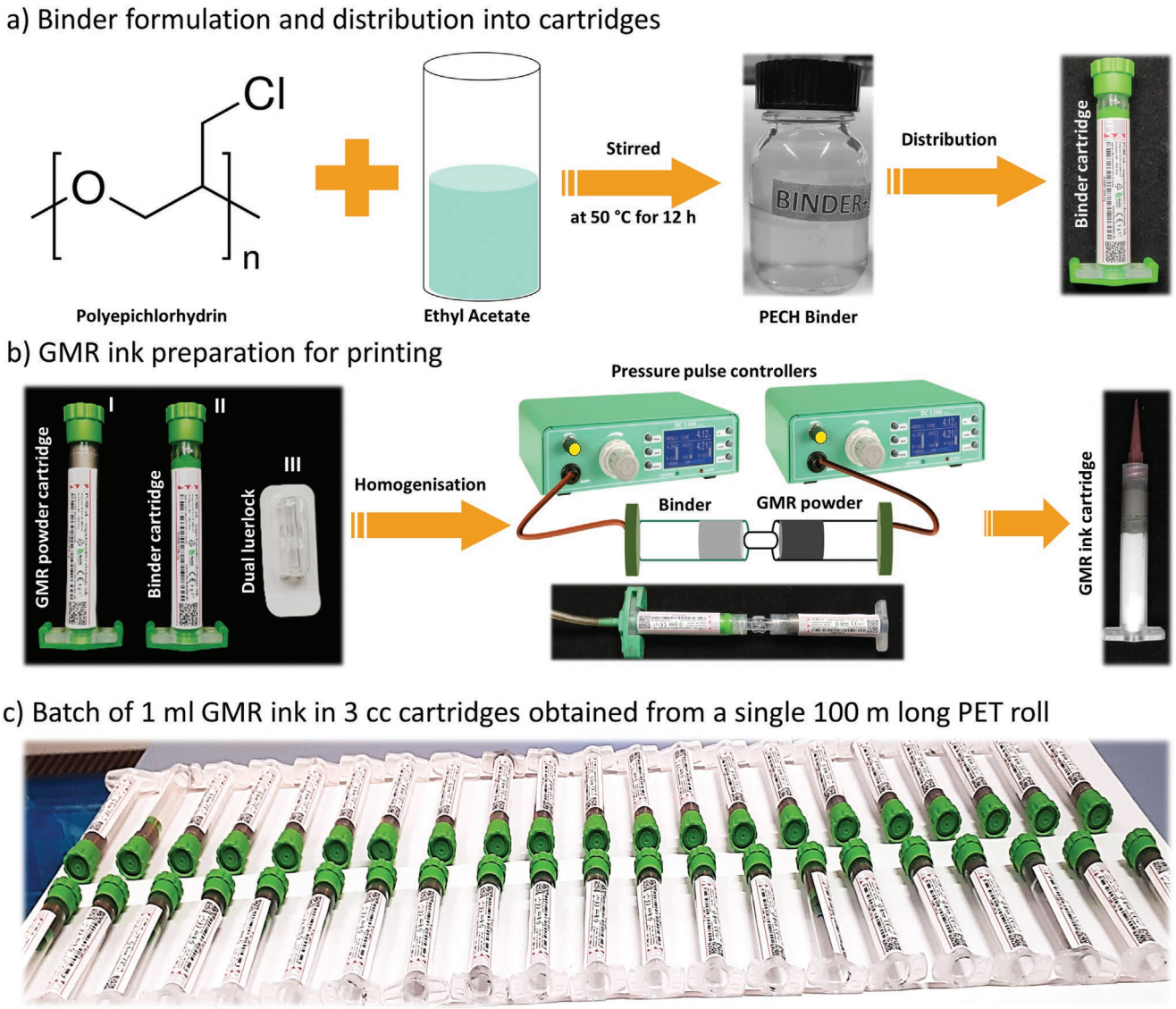


**Figure 4.** GMR ink preparation: a) Polyepichlorhydrin (PECH) polymer is mixed with ethyl acetate and stirred for 12 h at 50 °C to give final product and further loaded inside the cartridge and labeled as a binder cartridge. b) Magnetosensitive ink formulation: cartridge is loaded with weighed i) GMR powder and ii) PECH binder. iii) Dual luer-lock binds both cartridges for mixing and homogenization of the ink making the magnetosensitive (GMR) ink ready to use for printing. c) Represents the batch of 42 cartridges prepared from one single 100 m long magnetosensitive roll.

cartridge is loaded with the weighed amount of (Figure 4b-i) GMR powder (60 w%) (Figure 4b-ii) and connected to PECH binder (0.6 mL) (Figure 4b-iii) via a dual luer-lock connector to join the two cartridges for mixing and homogenization of the components. The binder and GMR powder cartridge are pressed with the digital dispenser (pulse pressure controller) forward and backward as shown in Figure 4b. The components are pushed out evenly by applying air pressure on one of the cartridges at a time, until the contents are uniformly blended and then transferred into one of the either cartridges with total final volume of ≈1 mL GMR ink. The 0.2 mm nozzle is then attached to the cartridge and GMR paste/ink is ready for dispense printing. The formulated GMR ink is used immediately or can be stored for later use. Similarly, 42 cartridges (3 cc) with GMR ink are (1 mL) prepared in one batch process from a 100 m magnetosensitive roll as shown in Figure 4c.

### 2.5. Printing Magnetoresistive Sensors

The arrays of silver contacts are printed on a thin flexible A4 size PET sheet by INKJET printing before printing magnetic sensors. Then, the magnetic sensors are printed by dispense printing using the prepared magnetosensitive ink (**Figure 5**a).

### 2.6. Magnetosensitive Ink Dispense Printing

The magnetosensitive ink is dispense printed using dispenseALL 420 system on a pre-printed Ag contact array (Figure 5b). The printing parameters of the dispense ALL tool have been optimized to obtain a smaller dot size of 1 mm with volume of 0.02 mL magnetosensitive ink being dispensed per sensor dot. The GMR ink is dispensed at the predefined positions and the cartridge head is moved from one position to the other with the coordinates mentioned in the recipe of the control software (Figure 5c). The complete 7 × 20 array is printed with magnetosensitive ink, whereas a total of three A4 PET's sheets can be printed with 1 mL ink loaded into the 3 cc cartridge. The dots are printed with the high accuracy on the predefined coordinates. The printed magnetoresistive sensor array is subjected to thermal treatment at 80 °C in order to remove excess of the solvent from the polymer binder, percolate and bind the magnetosensitive powder. The GMR performance of the printed 420 magnetoresistive sensors are then further evaluated collecting statistics on critical performance parameters.

### 2.7. Magnetoelectric Response of the Printed Magnetoresistive Sensors

The performance of the printed magnetoresistive sensors is assessed by measuring changes in electrical resistance with respect to the strength of an externally applied magnetic field. The magnetoelectric response of the printed sensor array is examined using a four- probe method. The magnetic field was swept in the range of ±1500 mT by an electromagnet. **Figure 6**a shows the magnetoelectric response of 140 printed GMR sensors, respectively for each flexible A4 size thin PET sheet, namely S1, S2, and S3. Out of 420 printed sensors 370 are operational, while 50 are misaligned with respect to the contacts lacking conductance and hence cannot be measured. The printed GMR sensor arrays showed the distribution in GMR ratio (Figure 6b) between ≈13% to ≈30% for S1, S2,

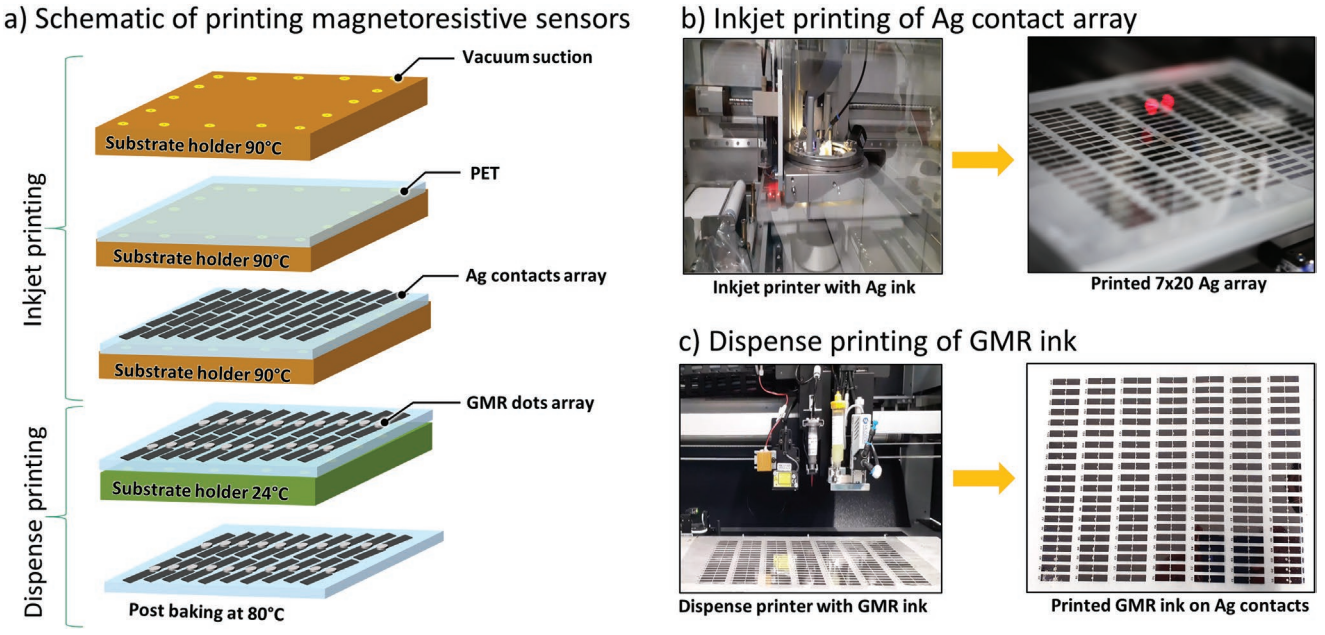


**Figure 5.** Magnetic sensors printing process. a) Schematic representation of printing process to achieve 7 × 20 array on the A4 size PET substrate. This process consists of inkjet printing of Ag contacts on hot 90 °C substrate holder and dispense printing of GMR sensors at room temperature with a final post printing backout process at 80 °C. b) Inkjet printing unit and the finished PET with an array of Ag printed contacts. c) Dispense printing unit and the substrate with finished printed magnetic sensors.

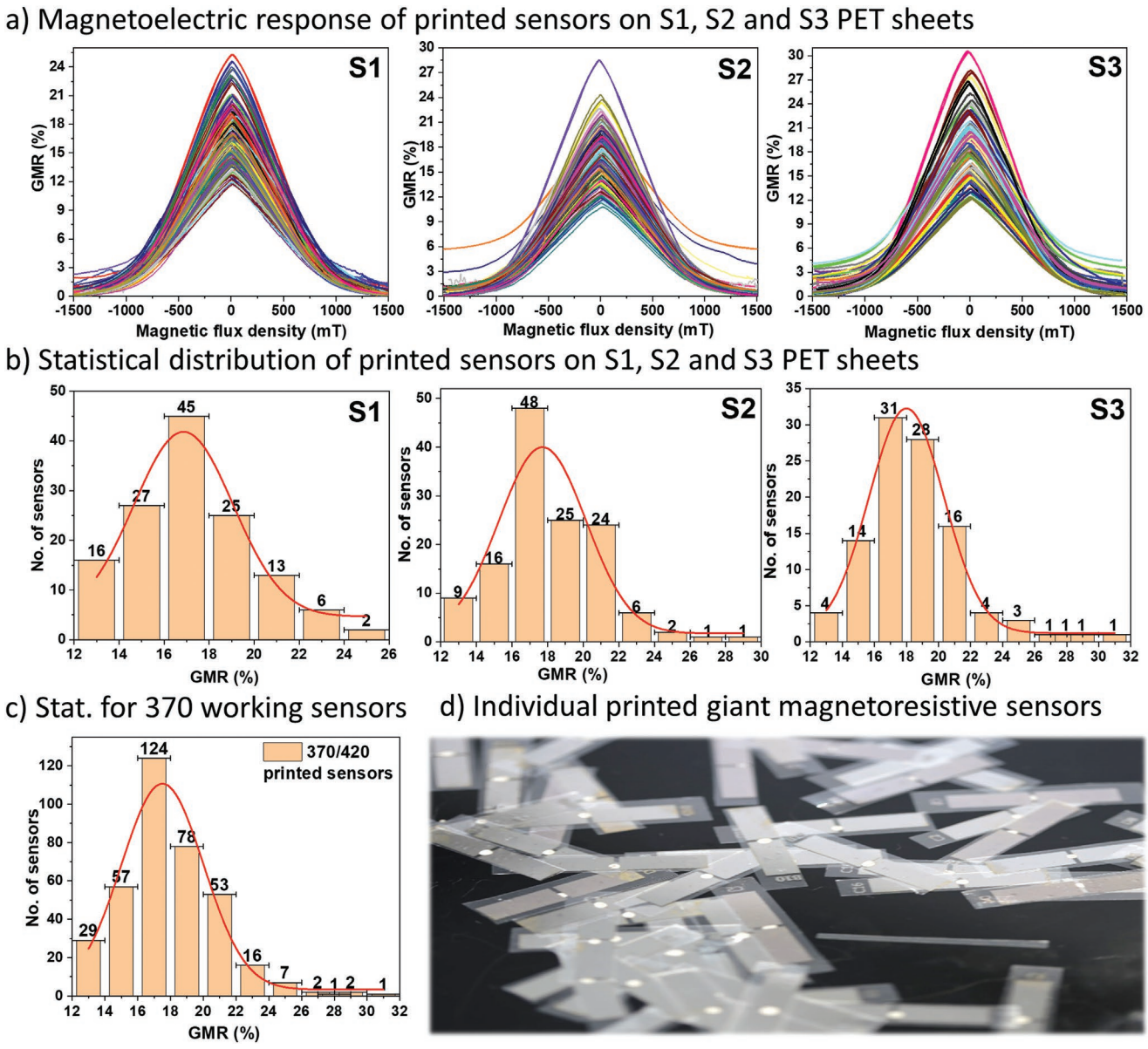


**Figure 6.** Characteristics of the printed magnetic sensors. a) Magnetoelectric response of 370 operating printed giant magnetoresistive sensors per each sheet S1, S2, and S3. b) Statistical distribution of the printed GMR sensors on S1, S2, and S3 PET sheets. c) Collective distribution of the 370 printed magnetoresistive sensors. d) Representative image of the individual printed magnetic sensors taken for magnetoelectric measurements.

and S3 with a maximum GMR response ranging between ≈18% and ≈20%. Statistically, the GMR effect can be concluded to be around 18% (Figure 6c) with the representative image of each of the printed sensors measured individually, as shown in Figure 6d. The saturation flux density for the printed sensors was measured to be about 1 T at room temperature, which is improved compared to our previous works (saturation field was about 2 T).[13,14] For a granular sensor system, the saturation field is about 5 T.[40] It can be attributed to the microstructure of the magnetosensitive powder having different GMR film flake sizes as obtained after the delamination process from PET foil. These different flake sizes have different responses to the magnetic field and average response of each individual flakes led to an increase in saturation field of the printed magnetoresistive sensors. The GMR effect observed in this work for printed magnetoresistive sensors fabricated on PET is significant (≈18%) in comparison to 4.5% and 6% on paper and silicon substrates previously observed by our group.[13] Recently, printable and stretchable magnetoresistive sensors are also demonstrated in $[Py/Cu]_{30}$ and $[Co/Cu]_{30}$ multilayer systems with low saturation field of 20 and 200 mT, respectively.[32] The high sensitivity observed in these system is indeed promising however the observed GMR effect (≈7%) is lower.[32] Nevertheless, the GMR response of the large-scale printed magnetoresistive sensors in this work is an important milestone in the field of printed magnetoelectronics as well as promising for realizing generalized precise functional thin-film layers on a large-scale.

## 3. Conclusion

In this work, we successfully demonstrated precise large-scale roll-to-roll fabrication of exchange coupled metallic multilayers for producing giant magnetoresistive thin-films. This enabled fabrication of relatively large application relevant quantities of the magnetosensitive material for printed electronics purposes. Large area manufacturing was achieved by a custom developed roll-to-roll, cassette based, modular physical vapor coating system, the enabling technology that is scalable and suitable for batch processing. We have shown that the fabrication of large area high quality exchange couple metallic multilayers on 100 m long and 0.2 m wide PET films can be accomplished with a significant GMR response of around 40%. This is a factor of around 10 000 increase in functional area of exchange coupled multilayers deposited in a single run and 150 times decrease in overall manufacturing time compared to previous reports. We have established the process to prepare magnetosensitive ink which is printable and achieves ≈18% of GMR value for the 370 printed magnetoresistive sensors made out of 1 mL ink. The significant value of GMR effect demonstrated in this work by the printed magnetoresistive sensors will contribute significantly to the design of future smart devices that are contactless, power efficient, and cost efficient. The development of the R2R deposition process and printed magnetoresistive sensors is a promising step toward economical and integrated magnetoelectronic systems. The obtained yield of magnetosensitive powder opens up the new avenue for realizing printable magnetoresistive sensors for hybrid magnetoelectronics. Importantly, this R2R approach is not limited to only one system and can also be utilized for other materials of interest in order to come in-line with the printed technology. This will open new fields of research, where precise but large-area manufacturing of functional materials is indispensable for instance for energy storage business and for biomedical applications to name a few.

## 4. Experimental Section

*Materials*: Co and Cu targets were purchased from EVOCHEM advanced materials. The Cu target was 99.99% pure with a dimension of $375 \times 132 \times 6$ mm$^3$. The Co target was 99.95% pure with the dimensions $371 \times 132 \times 3$ mm$^3$. Polyethylene terephthalate (PET) with the required dimension of $0.2 \times 100$ m$^2$ with the thickness of 50 µm was used as a substrate for depositing the metallic $(Co/Cu)_{30}$ multilayer. The PET web was purchased from UK insulations. The solvent Hexafluoroisopropanol (HFIP) was 99% pure and purchased from Fluorochem Limited, UK. Silver dispersion nanoparticle, 30–35 wt% in triethylene glycol monomethyl ether, spec. resistivity 11 $\mu\Omega$-cm, for printing on plastic films was purchased from Sigma-Aldrich. PECH polymer ($M_w$ 700 000) was purchased from Sigma-Aldrich Co. LLC. Ethyl acetate was purchased from VWR International, LLC and used without any further purification.

*Magnetoelectric Measurements of GMR Multilayer and Printed Sensor*: The four-point measurement configuration was employed for measuring the electrical response of the magnetosensitive roll and the printed magnetoresistive sensors with respect to an applied magnetic field. The sensor bias current was set to 1 mA, produced by a home-made constant current generator circuit, which was implemented directly into acquisition device. The Hall sensor measuring the magnetic field was connected to a parallel channel of the acquisition device. An electromagnet swept the magnetic field with a frequency of 1 Hz parallel or normal to the substrate. The voltage signals of both channels were simultaneously acquired, amplified, and adjusted to the input range of an analog-to-digital converter, embedded in the micro-controller unit (MCU) of the acquisition device. The data after processing in MCU, was sent via universal serial bus interface at a rate of 2000 measured points per second to a personal computer.

*Preparation of Binder Solution*: The binder was made up of PECH polymer (Sigma-Aldrich Co. LLC), $M_w$ 700 000 (1.4 g) in 20 mL solvent that is, ethyl acetate (VWR International, LLC). This binder solution was heated at 50 °C on hot plate and stirred at 400 rpm for 12 h to ensure complete and faster dissolution of polymer, till clear and transparent solution was obtained.

*Inkjet Printing of Ag Electrodes*: The A4 size PET foil was wiped and cleaned with Isopropyl alcohol (IPA) to ensure the surface was free from dirt or dust particle and further used as a substrate for printing Ag array. The $7 \times 20$ array of Ag electrode comprising two rectangles of dimension $15 \times 5$ mm was printed using LP50 inkjet printer. The Pixdro LP50 model had an A4 size substrate table with a vacuum pump and heating possibility up to 90 °C. The printing parameters were optimized for better printing quality microscopically. The Dimatix Materials Cartridges consisted of a fluid module which was filled with the ink and a jetting module (the printhead) with 16 nozzles arranged in one line with a nozzle distance of $snozzle = 254$ µm corresponding to a native resolution of $R = 100$ dpi. For this work, the cartridges DMC-11610 were used which had a nozzle diameter of 21 µm, ejected a nominal drop volume of 10 pL and could be operated at a maximum drop ejection of $f = 20$ kHz. The following parameters were set up for the printing: Cartridge temperature 45 °C, substrate temperature 90 °C, jetting frequency 925 Hz, applied voltage to piezoelectric inkjet head 45 V. All the 16 nozzles were set active. Resolution of inkjet printing was adjusted to 500 dpi by changing the cartridge mounting angle 1.1 to 90. The Ag ink used here was commercially available silver dispersion for printing on plastic films. The waveform was customized for printing the ink by controlling the drop formation and ejection via controlling electric signals and optimizing the printing parameters such as drop spacing, drop velocity, drop frequency, droplet size, and shape of the waveform. Initially, in order to move the piezoelectric element to relaxed position, the ink chamber was depressed with the bias voltage and then voltage is decreased to 0 V allowing it for the maximum volume. The ink was then pulled into the chamber for drop formation and chamber was further compressed to eject a drop. The waveform was optimized for piezo voltage to same bias level as standby mode preventing air bubbles from being sucked and clogging the print head after drop ejection. The printed Ag contacts were dried simultaneously by heating the substrate to temperature of 90 °C during printing and hence no further heat treatment was necessary. The printed Ag arrays showed low resistivity with values around 0.3 Ohm cm. This printed array was then used for further printing of magnetosensitive ink at defined preset positions between the Ag contacts.

*Magnetosensitive Ink Printing*: Followed by the inkjet printing of the Ag arrays, Fritsch dispense ALL 420 was used to print the GMR dots using formulated magnetosensitive ink. The dispense ALL had 2 dispensing valves with a universal carrier unit so that all could be used at the same time. Here, only 1 valve for printing magnetosensitive ink was used. The DA420 had a large working space along with set of magnetic holders which could be easily placed allowing the substrate enough height for dispensing. The robust metal sheet was used as a substrate holder for PET and locked up using the magnetic holders. The DA420 had a needle compensation and laser height sensor feature for precise dispensing from the cartridge and allowed it to produce same dosing position even after the cartridge change. The software allowed to load a printing receipt with the predefined coordinates for dispensing the magnetosensitive ink. A nozzle of the tip size was 0.2 mm, which was used for dispensing the ink and achieving a small dot size of 1 mm.

## Acknowledgements

The authors thank "VAKSIS R&D and Engineering" and Dr. Baybars Oral for the thoughtful discussions from designing to the final realization of R2R thin film deposition system. The authors thank C. Krien and I. Fiering (Leibniz IFW Dresden) for the support and help

in the laboratory. The authors also thank L. Schröder and C. Leger for the help in the laboratory. The authors thank C. Xu for the help in the laboratory and valuable discussions. The support in the development of the experimental setups from the research technology department of the Leibniz IFW Dresden and the clean room team headed by R. Engelhard (Leibniz IFW Dresden) is greatly appreciated. The authors acknowledge funding support from Leibniz Association (J21/2017 and T62/2019). This work was supported by the German Research Foundation DFG (Gottfried Wilhelm Leibniz Prize granted in 2018, SCHM 1298/22-1, KA5051/1-1 and KA5051/3-1).

Open access funding enabled and organized by Projekt DEAL.

## Conflict of Interest

The authors declare no conflict of interest.

## Data Availability Statement

The data that support the findings of this study are available from the corresponding author upon reasonable request.

## Keywords

giant magnetoresistance, large area deposition, magnetic ink, printed magnetoelectronics, roll-to-roll processing

Received: February 5, 2022
Revised: April 20, 2022
Published online:

[1] P. Grünberg, R. Schreiber, Y. Pang, U. Walz, M. B. Brodsky, H. Sowers, *J. Appl. Phys.* **1987**, *61*, 3750.
[2] M. N. Baibich, J. M. Broto, A. Fert, F. N. Van Dau, F. Petroff, P. Etienne, G. Creuzet, A. Friederich, J. Chazelas, *Phys. Rev. Lett.* **1988**, *61*, 2472.
[3] E. Y. Tsymbal, D. G. Pettifor, *Solid State Phys.* **2001**, *56*, 113.
[4] S. S. P. Parkin, *Annu. Rev. Mater. Sci.* **1995**, *25*, 357.
[5] I. Ennen, D. Kappe, T. Rempel, C. Glenske, A. Hütten, *Sensors* **2016**, *16*, 904.
[6] C. Giebeler, T. Kuiper, J. B. A. D. van Zon, M. Doescher, G. Schulz, D. Oelgeschlaeger, *Tech. Mess* **2001**, *68*, 215.
[7] J. Wecker, W. Clemens, E. Hufgard, *Mater. Sci. Forum* **1998**, *287–288*, 159.
[8] G. Rieger, K. Ludwig, J. Hauch, W. Clemens, *Sens. Actuators, A* **2001**, *91*, 7.
[9] M. J. Caruso, in *SAE International Congress and Exposition*, SAE International, Warrendale, PA **1997**, p. 9.
[10] D. R. Baselt, G. U. Lee, M. Natesan, S. W. Metzger, P. E. Sheehan, R. J. Colton, *Biosens. Bioelectron.* **1998**, *13*, 731.
[11] C. Zheng, K. Zhu, S. Cardoso de Freitas, J.-Y. Chang, J. E. Davies, P. Eames, P. P. Freitas, O. Kazakova, C. Kim, C.-W. Leung, S.-H. Liou, A. Ognev, S. N. Piramanayagam, P. Ripka, A. Samardak, K.-H. Shin, S.-Y. Tong, M.-J. Tung, S. X. Wang, S. Xue, X. Yin, P. W. T. Pong, *IEEE Trans. Magn.* **2019**, *55*, https://doi.org/10.1109/TMAG.2019.2896036.
[12] M. Melzer, D. Makarov, A. Calvimontes, D. Karnaushenko, S. Baunack, R. Kaltofen, Y. Mei, O. G. Schmidt, *Nano Lett.* **2011**, *11*, 2522.
[13] D. Karnaushenko, D. Makarov, C. Yan, R. Streubel, O. G. Schmidt, *Adv. Mater.* **2012**, *24*, 4518.
[14] D. Makarov, D. Karnaushenko, O. G. Schmidt, *ChemPhysChem* **2013**, *14*, 1771.
[15] J. A. Rogers, Z. Bao, K. Baldwin, A. Dodabalapur, B. Crone, V. R. Raju, V. Kuck, H. Katz, K. Amundson, J. Ewing, P. Drzaic, *Proc. Natl. Acad. Sci. USA* **2001**, *98*, 4835.
[16] J. A. Rogers, T. Someya, Y. Huang, *Science (80-.)*. **2010**, *327*, 1603.
[17] M. Kaltenbrunner, T. Sekitani, J. Reeder, T. Yokota, K. Kuribara, T. Tokuhara, M. Drack, R. Schwödiauer, I. Graz, S. Bauer-Gogonea, S. Bauer, T. Someya, *Nature* **2013**, *499*, 458.
[18] T. Sekitani, H. Nakajima, H. Maeda, T. Fukushima, T. Aida, K. Hata, T. Someya, *Nat. Mater.* **2009**, *8*, 494.
[19] G. A. Salvatore, N. Münzenrieder, T. Kinkeldei, L. Petti, C. Zysset, I. Strebel, L. Büthe, G. Tröster, *Nat. Commun.* **2014**, *5*, 2982.
[20] X. Wang, L. Dong, H. Zhang, R. Yu, C. Pan, Z. L. Wang, *Adv. Sci.* **2015**, *2*, 1500169.
[21] A. C. Arias, J. D. MacKenzie, I. McCulloch, J. Rivnay, A. Salleo, *Chem. Rev.* **2010**, *110*, 3.
[22] R. Abbel, Y. Galagan, P. Groen, *Adv. Eng. Mater.* **2018**, *20*, 1701190.
[23] S. H. Park, S. M. Lee, E. H. Ko, T. H. Kim, Y. C. Nah, S. J. Lee, J. H. Lee, H. K. Kim, *Sci. Rep.* **2016**, *6*, https://doi.org/10.1038/srep33868.
[24] J. Perelaer, P. J. Smith, D. Mager, D. Soltman, S. K. Volkman, V. Subramanian, J. G. Korvink, U. S. Schubert, *J. Mater. Chem.* **2010**, *20*, 8446.
[25] M. Singh, H. M. Haverinen, P. Dhagat, G. E. Jabbour, *Adv. Mater.* **2010**, *22*, 673.
[26] J. Wiklund, A. Karakoç, T. Palko, H. Yiğitler, K. Ruttik, R. Jäntti, J. Paltakari, *J. Manuf. Mater. Process.* **2021**, *5*, 89.
[27] P. Maiolino, M. Maggiali, G. Cannata, G. Metta, L. Natale, *IEEE Sens. J.* **2013**, *13*, 3910.
[28] N. Lu, D. H. Kim, *Soft Rob.* **2014**, *1*, 53.
[29] W. Gao, S. Emaminejad, H. Y. Y. Nyein, S. Challa, K. Chen, A. Peck, H. M. Fahad, H. Ota, H. Shiraki, D. Kiriya, D. H. Lien, G. A. Brooks, R. W. Davis, A. Javey, *Nature* **2016**, *529*, 509.
[30] J. C. Costa, F. Spina, P. Lugoda, L. Garcia-Garcia, D. Roggen, N. Münzenrieder, *Technologies* **2019**, *7*, 35.
[31] Q. Wei, J. H. Lee, K. W. Seong, M. N. Kim, J. H. Cho, *Biomed. Eng. Lett.* **2011**, *1*, 247.
[32] M. Ha, G. S. Cañón Bermúdez, T. Kosub, I. Mönch, Y. Zabila, E. S. Oliveros Mata, R. Illing, Y. Wang, J. Fassbender, D. Makarov, *Adv. Mater.* **2021**, *33*, 2005521.
[33] D. Karnaushenko, D. Makarov, M. Stöber, D. D. Karnaushenko, S. Baunack, O. G. Schmidt, *Adv. Mater.* **2015**, *27*, 880.
[34] E. Jansson, A. Korhonen, M. Hietala, T. Kololuoma, *Int. J. Adv. Manuf. Technol.* **2020**, *111*, 3017.
[35] M. B. Schubert, J. H. Werner, *Mater. Today* **2006**, *9*, 42.
[36] N. Palavesam, S. Marin, D. Hemmetzberger, C. Landesberger, K. Bock, C. Kutter, *Flexible Printed Electron.* **2018**, *3*, 014002.
[37] S. Tong, J. Yuan, C. Zhang, C. Wang, B. Liu, J. Shen, H. Xia, Y. Zou, H. Xie, J. Sun, S. Xiao, J. He, Y. Gao, J. Yang, *npj Flexible Electron.* **2018**, *2*, https://doi.org/10.1038/s41528-017-0020-y.
[38] M. Melzer, D. Karnaushenko, D. Makarov, L. Baraban, A. Calvimontes, I. Mönch, R. Kaltofen, Y. Mei, O. G. Schmidt, *RSC Adv.* **2012**, *2*, 2284.
[39] I. Colomer, A. E. R. Chamberlain, M. B. Haughey, T. J. Donohoe, *Nat. Rev. Chem.* **2017**, *1*, 0088.
[40] J. Q. Xiao, J. S. Jiang, C. L. Chien, *Phys. Rev. Lett.* **1992**, *68*, 3749.